Gmail

Kriengkri Timsorn <timsorn23@gmail.com>

Decision on your manuscript #JMSE-D-18-04138R1

1 message

Journal of Materials Science: Materials in Electronics (JMSE) <em@editorialmanager.com> Fri, Jan 18, 2019 at 5:49 PM
Reply-To: "Journal of Materials Science: Materials in Electronics (JMSE)" <pravin.selvakumar@springernature.com>
To: Kriengkri Timsorn <timsorn23@gmail.com>

You are being carbon copied ("cc:'d") on an e-mail "To" "Chatchawal Wongchoosuk" chatchawal.w@ku.ac.th
CC: safa.kasap.usask.ca@gmail.com, luojunjun32981@gmail.com, "Kriengkri Timsorn" timsorn23@gmail.com

Dear Dr. Wongchoosuk:

RE:
Title: "Inkjet printing of room-temperature gas sensors for identification of formalin contamination in squids"
Author(s): Kriengkri Timsorn; Chatchawal Wongchoosuk, Ph.D.
Accepted

I am pleased to tell you that this paper has been accepted for publication and is expected to appear in one of the forthcoming issues.

Sincerely yours,

Professor Jun Luo, Ph.D
Deputy Chief Editor
Journal of Materials Science: Materials in Electronics

Journal of Materials Science: Materials in Electronics
https://doi.org/10.1007/s10854-019-00772-9

Inkjet printing of room-temperature gas sensors for identification of formalin contamination in squids

Kriengkri Timsorn[1] · Chatchawal Wongchoosuk[2]

Received: 21 October 2018 / Accepted: 18 January 2019

Abstract

Printed room temperature gas sensors based on 2D hybrid pristine, NH_2 and N_2 functionalized multi-wall carbon nanotubes (MWCNTs)/PEDOT:PSS conductive polymer were fabricated by inkjet printing technique. The electronic inks prepared from MWCNTs dispersion in PEDOT:PSS were printed over interdigitated silver electrodes on flexible and transparent substrates. Surface morphology and functionalization of fabricated sensors were characterized by scanning electron microscopy (SEM) and Fourier transform infrared spectroscopy (FTIR). The sensing properties of hybrid printed films were exposed to various volatile organic compounds and gases including formaldehyde, ethanol, methanol, ammonia, nitrogen dioxide and hydrogen sulfide at room temperature. The results show that PEDOT:PSS/MWCNTs-N_2 sensor exhibits the highest sensitivity and selectivity to formaldehyde in concentration range of 10–200 ppm at room temperature. The sensing mechanism of the fabricated sensors can be explained based on charge transfer process and the interaction between functional groups of CNTS and formaldehyde molecules. The theoretical calculation based on self-consistent charge density functional tight-binding (SCC-DFTB) was employed and confirmed the proposed sensing mechanism. Moreover, a real-world food application of a fabricated sensor array was demonstrated through identification of formalin contamination in squids based on electronic nose and principal component analysis (PCA) method. The PCA shows the perfect classification between pure and formalin contaminated squid samples as well as different percentages of contaminations.

1 Introduction

Addition of formalin to seafood due to spoilage prevention is one of crucial problems for the food industry in Thailand and many countries. Assessment of formaldehyde (gas phase of formalin) has become a quick method instead of a typical chemical process for identification of formalin contamination in seafood. Formaldehyde is a colorless, flammable and reactive gas that causes damage to human health including high rate of cancer, respiratory illness, immune system disorder, central nervous system damage and children abnormalities etc. [1–5]. World Health Organization (WHO) and International Agency for Research on Cancer have also classified formaldehyde as a human carcinogen [6, 7]. Therefore, it is very necessary to accurately monitor formaldehyde for the safety and quality of seafood. Nowadays, several researcher groups have developed the systems and gas sensors to detect formaldehyde contamination in food. However, most employed gas sensors for formaldehyde detection were commercial metal oxide gas sensors that need high operating temperatures (200–400 °C) [8–10] and they always exhibit cross sensitivity problems.

Recent decades, nanomaterials based gas sensors have been extensively investigated for formaldehyde detection [4, 5, 11–15]. Carbon nanotubes (CNTs) are considered as one of the best sensing materials for gas sensors due to their unique properties including ultrahigh surface area, high electron mobility, good electronic properties, surface modification and functionalization etc. [16–20]. CNTs have been successfully used to detect various gases such as NO_2 [21, 22], NH_3 [23, 24] and O_2 [25]. For formaldehyde detection, CNTs were found to be low sensitivity and selectivity to formaldehyde because of weak physical adsorption

Electronic supplementary material The online version of this article (https://doi.org/10.1007/s10854-019-00772-9) contains supplementary material, which is available to authorized users.

✉ Chatchawal Wongchoosuk
chatchawal.w@ku.ac.th

1 Physics division, Faculty of Science and Technology, Phetchabun Rajabhat University, Phetchabun 67000, Thailand

2 Department of Physics, Faculty of Science, Kasetsart University, Chatuchak, Bangkok 10900, Thailand

Published online: 23 January 2019

(van der Waals force) between CNTs and formaldehyde molecules [12, 26]. To enhance the sensitivity of CNTs for formaldehyde adsorption, CNTs were functionalized with Ag–$LaFeO_3$ [12] and amino groups [11].

Poly(3,4-ethylenedioxythiophene):poly(styrenesulfonate) (PEDOT:PSS) is a conductive polymer that widely used for printed electronics due to its good conductivity, reproducibility, high transparency, and processability [27, 28]. However, PEDOT:PSS has limited structural and chemical properties that still remain as major obstacles for its practical sensing applications. To compare the sensing performances with other 2D thin-layered nanomaterials such as MoS_2 [29] black phosphorus [30] $SnSe_2$ [31] etc. [32], pure PEDOT:PSS gave a low sensitivity towards gases and volatile organic compounds (VOCs). Combination of PEDOT:PSS with novel carbon nanostructures is a potential solution to enhance the sensitivity and selectivity of such sensors [33].

In this work, we have investigated the sensing capabilities of hybrid CNTs/poly(3,4-ethylenedioxythiophene):poly(styrenesulfonate) (PEDOT:PSS) with respect to formaldehyde at room temperature. The nanocomposites between CNTs and PEDOT:PSS are expected to provide good performance of gas sensing response due to rich of charge carriers. Three different gas sensors including PEDOT:PSS/pristine MWCNTs, PEDOT:PSS/MWCNTs-NH_2 and PEDOT:PSS/MWCNTs-N_2 were fabricated via a low-cost inkjet printing method. It should be noted that advantages of these 2D hybrid films for sensors include flexibility, room temperature fabrications, simplicity, low cost, and good stability. The sensing mechanism of the fabricated sensors and effects of NH_2 and N_2 functionalization were investigated by self-consistent charge density functional tight-binding (SCC-DFTB) method. The real-world application of the room-temperature gas sensors was demonstrated through identification of formalin contamination in squids based on electronic nose technique.

2 Experimental procedures

2.1 Sample preparation

Fresh squids were purchased from a local market in Bangkok, Thailand. They were immediately packed in commercial food grade plastic bags and stored in a container at 4.0 °C without cleaning. Formalin contamination of samples was obtained by dipping squid samples (weight of 20–30 g) in formalin (2.5 wt%, 1 wt%, and 0.125 wt%) mixed with DI water solution of 200 ml. It should be noted that the smell of this selected formalin concentrations in DI water cannot be detected by human nose. Each sample was dipped in the formalin solutions for 1 h at room temperature. Then, the squids were washed with clean water and kept in the sample glass bottles for further measurements.

2.2 Preparation of electronic ink

MWCNTs (outer diameter = 20–30 nm, length = 10–30 μm, purity > 95 wt%), MWCNTs-NH_2 (outer diameter = 13–18 nm, length = 3–30 μm, purity > 99 wt% and functional content = 7.0% ± 1.5%) and MWCNTs-N_2 (outer diameter = 13–18 nm, length = 3–30 μm, purity > 99 wt% and functional content = 7.0% ± 1.5%) were purchased from Cheap Tubes Inc. It should be noted that this dimension difference did not cause any significant effects on sensing performance of the final printed sensors as displayed in Fig. S1 in the Supplementary Information.

PEDOT:PSS aqueous solution (Clevios™ P VP AI 4083, solid content 1.3–1.7%, weight ratio 1:6) was obtained from Heraeus Deutschland GmbH & Co., KG. *N,N*-Dimethylformamide (DMF), dimethyl sulfoxide (DMSO), ethylene glycol (EG) and triton X-100 were purchased from Sigma-Aldrich and used without any further purification. Firstly, 200 mg of each MWCNTs sample was dispersed in 20 ml of DMF solution and sonicated for 20 min in order to obtain good dispersion of MWCNTs in DMF solution. Then, the suspensions were centrifuged for 15 min at 3000 rpm to remove large particle aggregates. The concentrations of suspensions were approximately 10 mg/ml. Next, PEDOT:PSS of 90% weight concentration was dissolved in a mixture solvent containing 5 wt% of DMSO, 2.5 wt% of EG and 2.5 wt% of triton X-100. DMSO was used for enhancing the cohesion and electrical conductivity of PEDOT:PSS electronic ink while EG and TX-100 were added for improvement of viscosity and surface tension to avoid a rapid drying and clogging in the printer head. The final viscosity and surface tension of formulated inks measured by Brookfiel Viscometer and Kurss Tensiometer were in the range of 10–12 cPs and 40–45 mN/m respectively. Homogeneous solution of PEDOT:PSS with the mixture solvent was obtained by magnetically stirring for 20 min at room temperature. In preparation of conductive sensing ink, each suspension was mixed with homogeneous PEDOT:PSS solution with a suspension to PEDOT:PSS solution volume ratio of 2:3. Finally, the obtained electronic ink was magnetically stirred for 1 h at room temperature.

2.3 Fabrication of gas sensors by inkjet printing

The silver conductive paste was deposited on a transparent and flexible substrate by screen printing to form interdigitated electrodes with 1 mm interdigited spacing and rectangular area of 1.5×2.5 cm^2 (see Fig. 1a). The inkjet printer cartridge (HP 61 black ink cartridge) was rinsed with DI water by ultrasonication and dried in air. The prepared

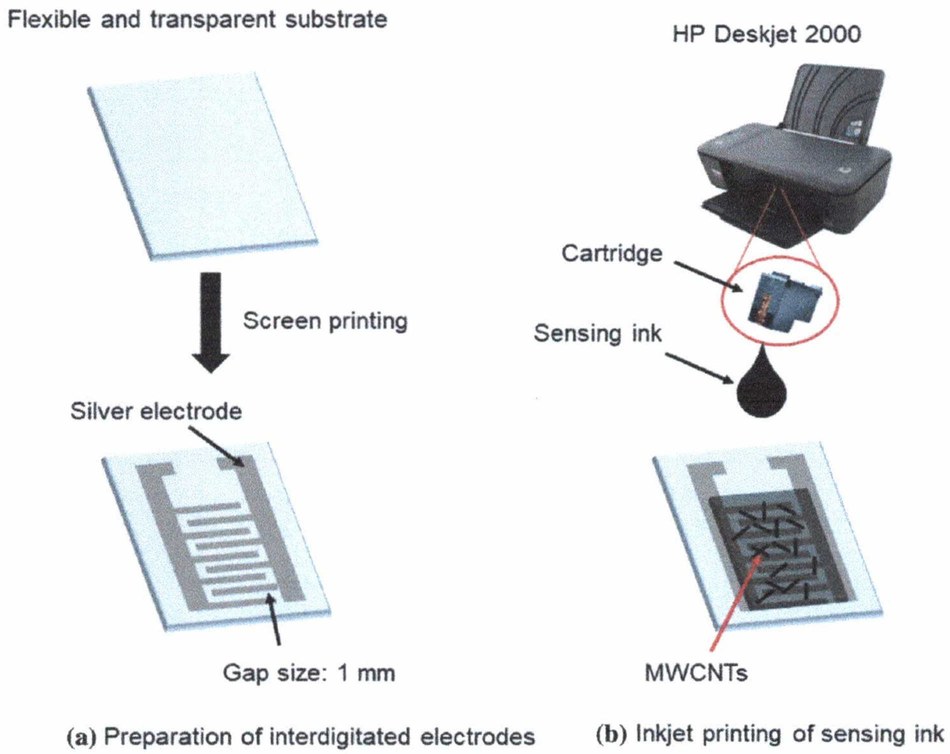

Fig. 1 Schematic diagram of gas sensor fabrication

sensing ink was filled into the cleaned cartridge and then directly printed over silver electrodes on the substrate using HP deskjet 2000 j210 printer in single mode with resolution of 1200 × 1200 dpi, as shown in Fig. 1b. After each printing, the printed sensing ink on the substrate was dried by an air blower at room temperature for 10 min. It should be noted that the printed sensing layer did not totally dried at this stage but the rigidity of the printed layer was good enough for the next printed layers. The thickness of printed sensing films could be controlled by overwriting of sensing ink on the substrate. The sensing films were obtained by six times overwriting. The final thicknesses of the printed PEDOT:PSS/MWCNTs, PEDOT:PSS/MWCNTs-N_2 and PEDOT:PSS/MWCNTs-NH_2 are ~ 249 nm ~ 255 nm and ~ 252 nm, respectively.

2.4 Gas sensing measurement

The gas sensing properties of the fabricated gas sensors were measured towards different test gases including formaldehyde, ethanol, methanol, ammonia, nitrogen dioxide and hydrogen sulfide at room temperature. The test gas sources at different flow rate ratios were mixed with a constant flux of synthetic air to obtain desired concentrations using mass flow controllers. The total flow rate was fixed at 2 l/min. Each test gas was delivered to the sensors in a test chamber for 2 min. After gas exposure, the sensors were cleaned with the cleaned air for 2 min. All experiments were performed at room temperature (25 ± 2 °C) in dry air. The changes in sensor resistances were recorded every second using LabVIEW with NI USB DAQ 6008. The sensor responses can be calculated as $S(\%) = [(R_{air} - R_{gas})/R_{air}] \times 100$, where R_{air} and R_{gas} are sensor resistance values in air (baseline resistance) and gas exposure, respectively.

2.5 Measurement of formalin contamination in squids

To identify formalin contamination in squids, the fabricated gas sensors (PEDOT:PSS/MWCNTs, PEDOT:PSS/MWCNTs-NH_2 and PEDOT:PSS/MWCNTs-N_2) were installed in a Teflon chamber in our lab-made electronic nose (E-nose) system. Figure 2 shows schematic diagram of our E-nose system. To start a measurement, air was pumped passing an activated carbon bottle into a mass flow controller at a flow rate of 2 l/min. Clean air from the reference bottle was carried into the sensor chamber for 2 min in order to obtain baseline resistances of sensors. After 2 min, valves 1 and 2 were closed and valves 3 and 4 were opened at the same time. Air flow path was switched to the sample bottle. Volatile organic compounds generated from headspace of squid samples were carried into the sensor chamber for 2 min. The change in sensor resistances was recorded every second as

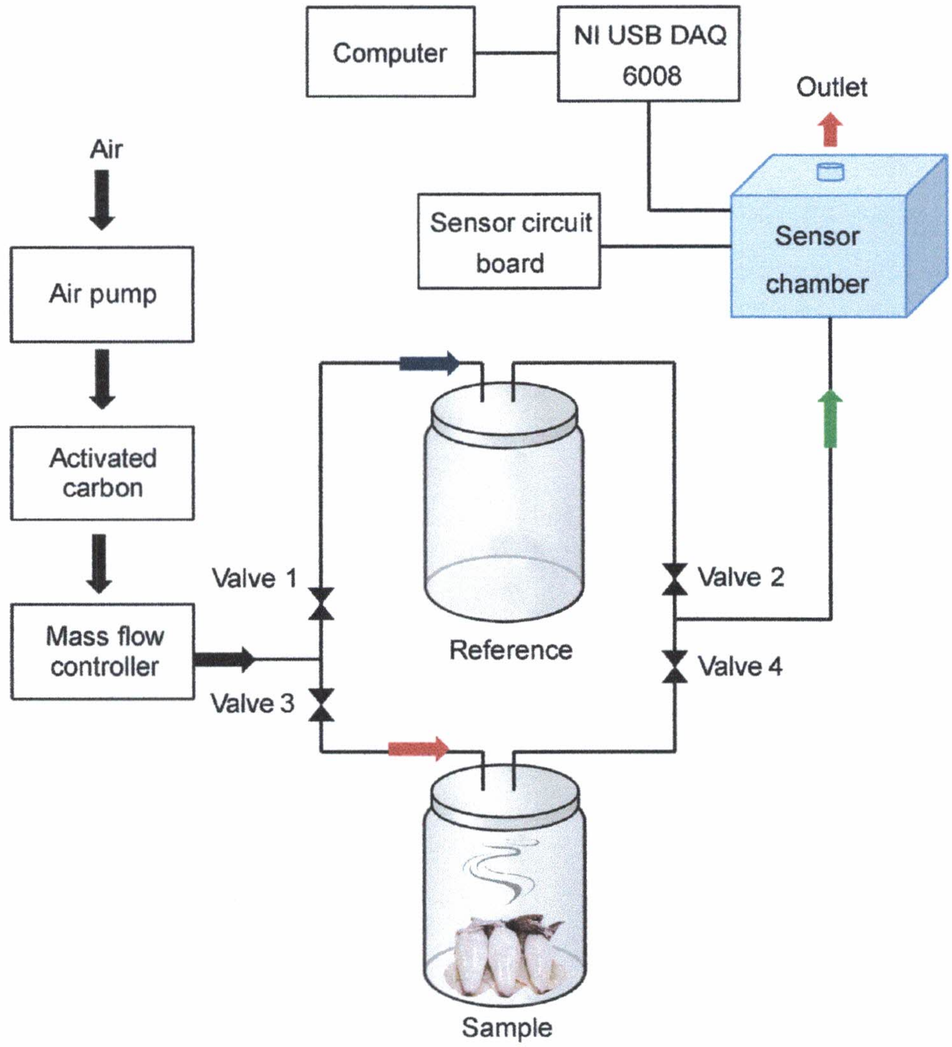

Fig. 2 Our lab-made E-nose system for measurement of formalin contamination in squids

a function of time. All devices in the E-nose system were controlled via our LabVIEW programming.

2.6 Principal component analysis (PCA)

PCA is a well-known statistical method that has been widely used for data classification in various applications as well as food quality control [34–40]. The purpose of PCA is to reduce dimensionality of numerical data sets with retaining the most of information [35, 38, 41–43]. It converts a data set of correlated variables into a set of uncorrelated variables using an orthogonal transformation. Each data set of uncorrelated variables is called principal components (PCs). The first principal component (PC1) contains the largest percentage of total variance. The second largest percentage is on the second principal component (PC2), and so on. The obtained new data sets are plotted and classified on two or three dimensions to visually estimate the similarities and differences between samples [44]. The PCA result can be calculated as the following equation [34, 35, 38]:

$$PCA = \left((\overrightarrow{Cov(X_{M \times N})})_{max \to min} \otimes Norm(X_{M \times N}) \right)^{T} \quad (1)$$

where Cov ($X_{M \times N}$) is covariance matrix and T is transpose. M and N represent the different repetitions of measurement and a number of independent sensors, respectively. Norm is normalization of data matrix.

2.7 Self-consistent charge density functional tight-binding (SCC-DFTB) method

The theoretical studies of adsorption behaviors of formaldehyde molecules (HCHO) on pristine and functionalized carbon nanotubes were performed using the SCC-DFTB method. It should be noted that the SCC-DFTB method was derived from density functional theory (DFT) based on a second-order expansion of the DFT total energy expression [45–48]. Both pristine and functionalized CNTs with length of 20 Å and diameter of 7.15 Å were selected. Carbon atoms at the tube ends were saturated with hydrogen atoms to reduce boundary effects [47]. Adsorption distances between pristine and functionalized SWCNTs and HCHO molecules were varied. The adsorption energy (E_{ad}) is defined as:

$$E_{ad} = E_{tot}(CNTs + HCHO) - E_{tot}(CNTs) - E_{tot}(HCHO) \quad (2)$$

where E_{tot} (CNTs + HCHO), E_{tot} (CNTs) and E_{tot} (HCHO) are the total energies of CNTs with HCHO molecules system, individual CNTs models, and individual HCHO molecule, respectively.

3 Results and discussion

3.1 Characterization of sensing films

The surface morphology and microscopic structure of the printed sensing films were characterized by scanning electron microscope (SEM). Figure 3a shows a portion of interdigitated silver electrodes with 1 mm interdigited spacing. The SEM images of pure PEDOT:PSS, PEDOT:PSS/MWCNTs, PEDOT:PSS/MWCNTs-N_2 and PEDOT:PSS/MWCNTs-NH_2 sensing film surfaces are illustrated in Fig. 3b–e, respectively. It can be seen that the printed pure PEDOT:PSS sensing film is quite smooth with very low defect. It refers to obtain high homogenous sensing films based on our electronic ink formula with low-cost inkjet printing method. In case of hybrid PEDOT:PSS/CNTs, both pristine and functionalized MWCNTs are in the form of bundles in PEDOT:PSS matrix. No significant surface morphological differences can be observed among the different functional groups and pristine one. It indicates that functionalization of CNTs did not provide a surface area enhancement but functional groups may help to increase the interactions to targeted gas molecules.

To confirm the existence of N_2 and NH_2 functional groups in the printed sensing films, Fourier transform infrared spectroscopy (FTIR) was performed to analyze the bonds between MWCNTs and functional groups. Figure 4 demonstrates FTIR spectra of printed PEDOT:PSS/MWCNTs, PEDOT:PSS/MWCNTs-N_2 and PEDOT:PSS/MWCNTs-NH_2 sensing films. When MWCNTs are well embedded in PEDOT:PSS matrix, PEDOT:PSS polymer chains can thus adsorb to the surface of the MWCNTs. Main peaks of these composite sensing materials contribute from PEDOT:PSS [33]. The vibrational bands at 1650, 2910 and 3383 cm^{-1} are assigned to C=O stretching, C–H stretching and O–H in the carboxyl group stretching vibrational modes [11, 33, 49–51], respectively. The spectra of PEDOT:PSS/MWCNTs-N_2 and PEDOT:PSS/MWCNTs-NH_2 sensing films similarly contain vibrational bands of C–N (graphitic) at 1018 cm^{-1} and N–H (pyrrolic) at 917 and 921 cm^{-1} for PEDOT:PSS/MWCNTs-N_2 and PEDOT:PSS/MWCNTs-NH_2 [50–53], respectively. In the case of PEDOT:PSS/MWCNTs spectrum, there is no

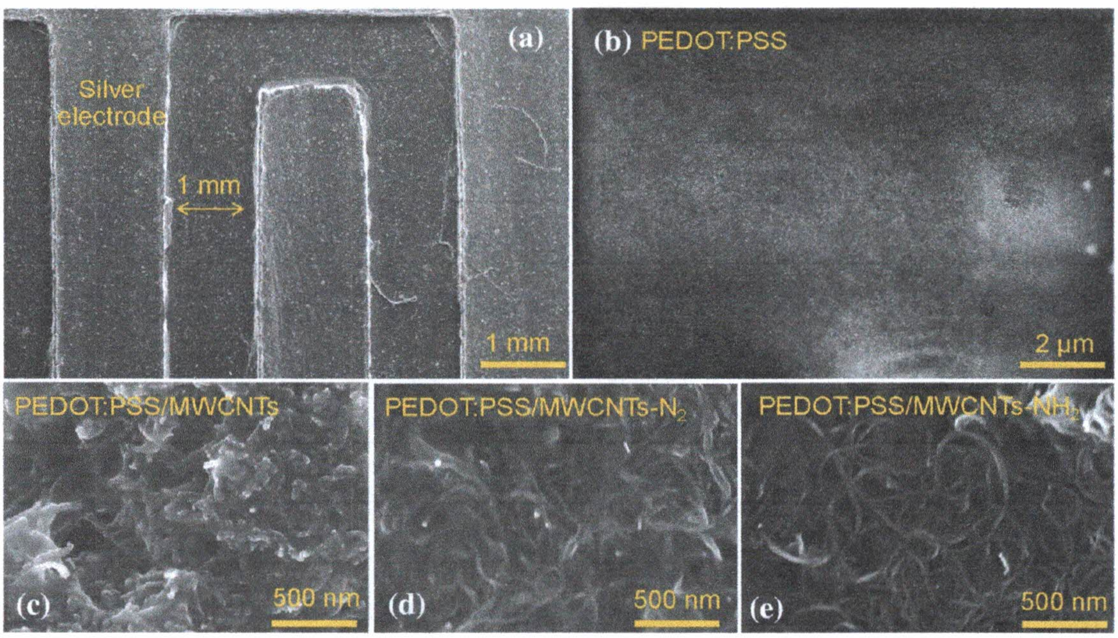

Fig. 3 SEM images of **a** interdigitated silver electrode and printed **b** pure PEDOT:PSS, **c** PEDOT:PSS/MWCNTs, **d** PEDOT:PSS/MWCNTs-N_2, and **e** PEDOT:PSS/MWCNTs-NH_2 sensing films on silver electrodes

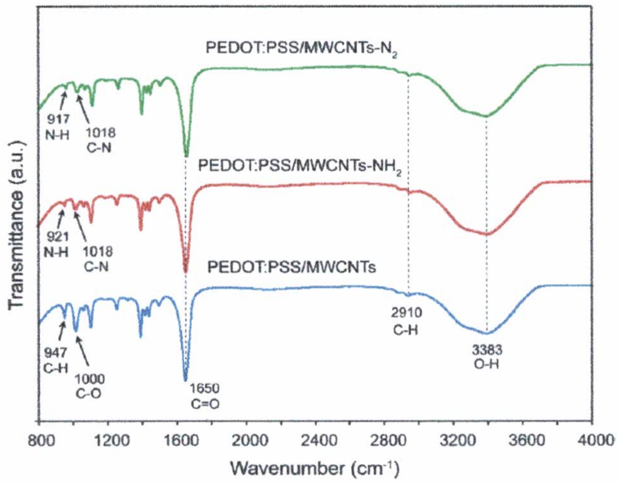

Fig. 4 FTIR spectra of PEDOT:PSS/MWCNTs, PEDOT:PSS/MWCNTs-N_2 and PEDOT:PSS/MWCNTs-NH_2 sensing films

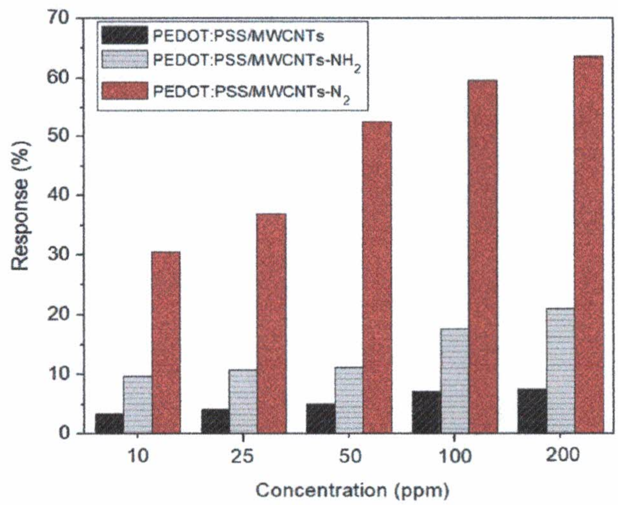

Fig. 5 The responses of three printed gas sensors to formaldehyde gas with different concentrations at room temperature

appearance of C–N and N–H vibrational bands. The presence of C–N and N–H vibrational bands in the spectra of PEDOT:PSS/MWCNTs-N_2 and PEDOT:PSS/MWCNTs-NH_2 sensing films confirms the existence of N_2 and NH_2 molecules on MWCNTs surfaces after printing by our low-cost inkjet printing method.

3.2 Gas sensing properties

Figure 5 depicts the response of three printed gas sensors to formaldehyde gas with different concentrations of 10, 25, 50, 100 and 200 ppm at room temperature. It can be clearly seen that the PEDOT:PSS/MWCNTs-N_2 gas sensor exhibits the highest response to formaldehyde at room temperature. Especially for 10 ppm formaldehyde concentration, the responses of PEDOT:PSS/MWCNTs-N_2, PEDOT:PSS/MWCNTs-NH_2 and PEDOT:PSS/MWCNTs gas sensors are 30.5%, 9.7% and 3.4%, respectively. The response of PEDOT:PSS/MWCNTs-N_2 to formaldehyde gas is about three times that of PEDOT:PSS/MWCNTs-NH_2 and ten times that of PEDOT:PSS/MWCNTs at room temperature. In addition, the response of the three gas sensors increases with increasing formaldehyde concentrations. It is seen that the functionalization of N_2 molecules on MWCNTs surfaces improves better response to formaldehyde gas. The average resistances of PEDOT:PSS/MWCNTs, PEDOT:PSS/ MWCNTs-N_2 and PEDOT:PSS/MWCNTs-NH_2 sensors in pure air are ~ 6.46 kΩ, ~ 35.12 kΩ, and ~ 40.27 kΩ, respectively (see Fig. S2 in the Supplementary Information). The response and recovery times of the printed sensors are defined as the time required for the sensor resistance to reach 90% of the final equilibrium value upon gas injection and air recovery, respectively. The response times of PEDOT:PSS/MWCNTs-N_2, PEDOT:PSS/MWCNTs-NH_2 and PEDOT:PSS/MWCNTs gas sensors are estimated to be 45 s, 48 s and 55 s, respectively while all sensors exhibit the similar recovery times (~ 7 s). Dynamic response of PEDOT:PSS/functionalized MWCNTs sensors is better than PEDOT:PSS/pure MWCNTs sensor and other sensing materials for formaldehyde detection at room temperature [11, 54, 55]. The limit of detection of the PEDOT:PSS/MWCNTs-N_2 gas sensor is found to be 1 ppm at room temperature while the detection limits for PEDOT:PSS/MWCNTs and PEDOT:PSS/MWCNTs-NH_2 sensors are 10 ppm and 5 ppm, respectively. The printed sensor based on PEDOT:PSS/MWCNTs-N_2 exhibits much lower formaldehyde detection limit also. The sensing mechanism and functionalization effect of the three gas sensors will be discussed in the next section.

To investigate the selectivity of three printed gas sensors, they were exposed to 200 ppm concentrations of ethanol, methanol, ammonia, nitrogen dioxide and hydrogen sulfide at room temperature as shown in Fig. 6. It is found that the response of PEDOT:PSS/MWCNTs without functionalization exhibits very low response of 8.5%, 7.5%, 5.8%, 5.3%, 3.21% and 1.78% to formaldehyde, ammonia, methanol, ethanol, nitrogen dioxide and hydrogen sulfide, respectively. For functionalization, the PEDOT:PSS/MWCNTs-N_2 and PEDOT:PSS/MWCNTs-NH_2 sensors show a significant improvement of sensor responses to formaldehyde and ammonia. One can be seen that PEDOT:PSS/MWCNTs-N_2 sensor owns a high sensitivity and selectivity to formaldehyde at room temperature over other gases. This results from higher percentage of N molecules in sensing film corresponding to a previous publication [11]. They can help to increase donor–acceptor interactions and charge transfers of formaldehyde adsorption on the host material. In addition,

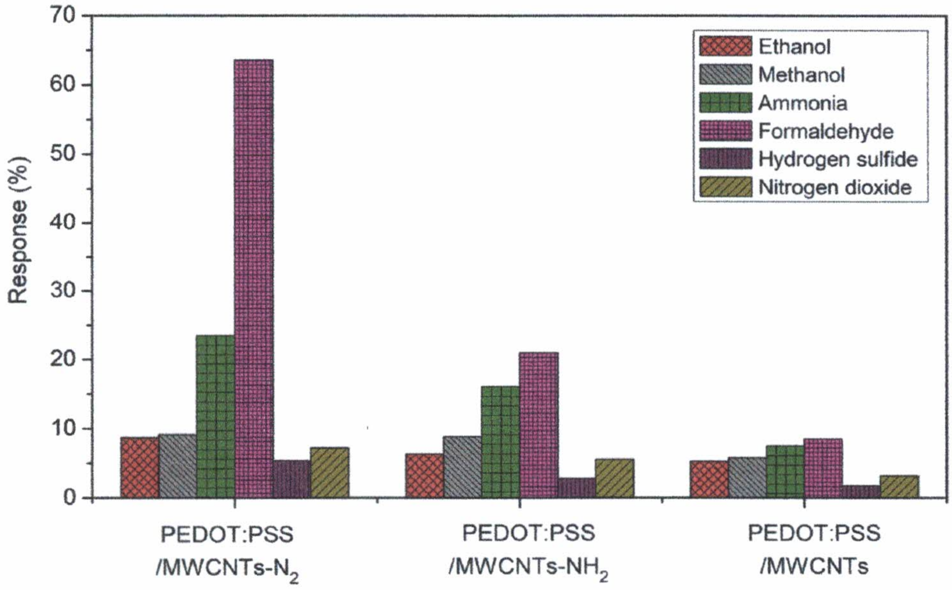

Fig. 6 The selectivity of three printed gas sensors to various gases at 200 ppm concentration

PEDOT:PSS/MWCNTs-N_2 sensor also exhibits a good repeatability. The resistance of the sensor decreases upon exposure to formaldehyde and return to the initial value upon the removal of formaldehyde in air upon 5 cycles with SD of sensor responses ~ 0.89% as displayed in Fig. S3 in the Supplementary Information.

3.3 Sensing mechanism of fabricated sensors

All printed gas sensors decrease in the sensor resistances with exposure of formaldehyde at room temperature as shown in Fig. S2 in the Supplementary Information. Formaldehyde is electron donating gas [56]. When formaldehyde molecules are adsorbed on PEDOT:PSS/CNTs surface, electrons are transferred to the composites. In our case, the hybrid PEDOT:PSS/CNTs gas sensors behave as n-type nanomaterials in which the carrier concentration increases upon the introduction of electron donating gases. To investigate the different sensing properties of three printed gas sensors, SCC-DFTB method was employed for theoretical study of formaldehyde adsorption on pristine, N_2 and NH_2 functionalized CNTs. It should be noted that PEDOT:PSS did not included in simulations because it acts as a host material for all sensors. To simplify the model, only different CNTs were used to study the interactions with formaldehyde molecule. To find the most favorable adsorption configuration, a formaldehyde molecule was placed at different distances (d) above the nanotubes as displayed in Fig. 7a. The adsorption energy was calculated and plotted as a function of the distances as shown in Fig. 7b. The highest adsorption energies of CNT, CNT-NH_2 and CNT-N_2 are − 0.0520 eV, − 0.0995 eV and − 0.1266 eV, respectively, at the similar distance of 3.0 Å. Before formaldehyde adsorption, the Fermi energy levels relative to the vacuum level of CNT, CNT-NH_2 and CNT-N_2 are − 4.382 eV, − 4.327 eV and − 4.248 eV, respectively, while the energy gaps of CNT, CNT-NH_2 and CNT-N_2 are 0.4402 eV, 0.2295 eV and 0.2003 eV respectively. It should be noted that the energy gaps were estimated from difference in energy between the lowest unoccupied molecular orbital (LUMO) and the highest occupied molecular orbital (HOMO). After adsorption, the corresponding Fermi energy levels are shifted to − 4.391 eV, − 4.370 eV and − 4.304 eV, respectively, while the energy gaps reduce to 0.4401 eV, 0.2201 eV and 0.1952 eV, respectively. These results indicate that the Fermi energy levels shift downward after formaldehyde adsorption and CNT-N_2 exhibits the largest shift in Fermi energy level and energy gap reduction. The SCC-DFTB results show a good agreement with experimental results. The N_2 functionalization enhances better response to formaldehyde gas over pristine and NH_2 functionalized carbon nanotubes. In addition, electron charge transfer was found to be from the formaldehyde molecule to the CNT-N_2 (0.079e) at the optimum adsorption site of 3.0 Å. The CNT-N_2 interacts with the electron-donating formaldehyde resulting to increase in charge carriers of CNT-N_2. It causes the decrease in resistance of sensing film in present of formaldehyde.

3.4 Identification of formalin contamination in squids based on PCA analysis

To apply the fabricated room-temperature gas sensors in real-world application, three sensors (PEDOT:PSS/MWCNTs-N_2, PEDOT:PSS/MWCNTs-NH_2 and PEDOT:PSS/MWCNTs gas sensors) were installed in the E-nose and used for identification of formalin contamination in squids.

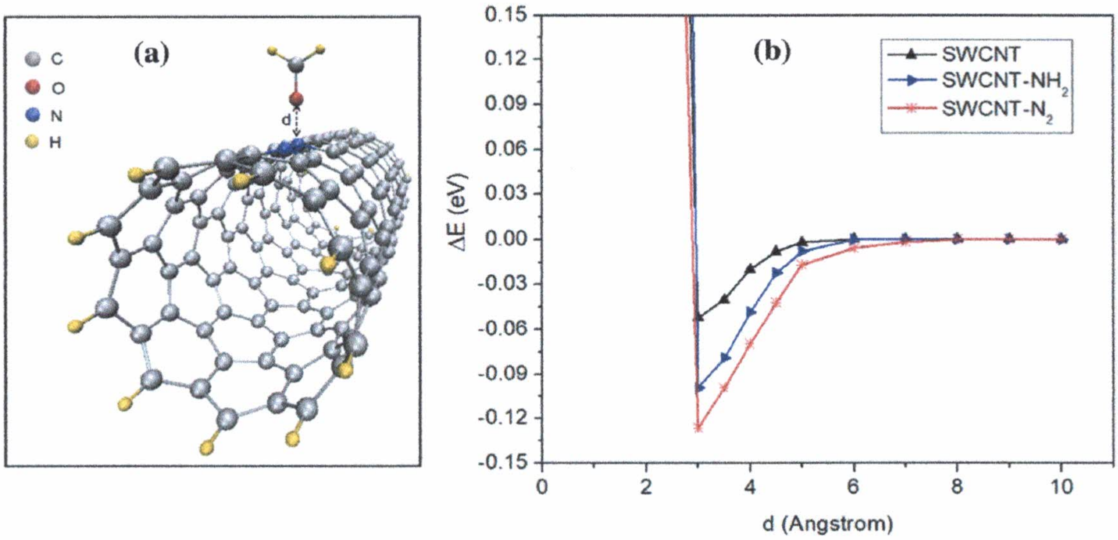

Fig. 7 **a** Model of interaction between CNT-N_2 and a formaldehyde molecule and **b** adsorption energy as a function of adsorption distance

180 sensor responses ($X_{60\times3}$) were introduced into the PCA analysis. Figure 8 presents 2D PCA plot of four different squid samples at room temperature. The PC1 contributes 96.85% of the total variance and the PC2 contains 2.07% of the total variance. The cumulative of the PC1 and PC2 represents 98.92% of data variance which provides high enough information to describe the odor difference of pure and formaldehyde contaminated squid samples. From Fig. 8, it can be clearly seen that the PCA result shows a perfect classification of four sample groups corresponding to the percentages of formalin contamination (pure, 0.125 wt%, 1 wt% and 2.5 wt%). Moving along the PC1 axis from left to right, the sample groups with higher formalin contamination distribute further from the pure sample group. This suggests the obvious difference in odors of squid samples contaminated with different concentrations of formalin contamination. In addition, the difference of squid samples dipped in formalin mixed DI water solution cannot be detected from physical observation as shown in inset of Fig. 8. The PCA result confirms that our inkjet-printed gas sensor array has

Fig. 8 PCA plot for classification of squid samples

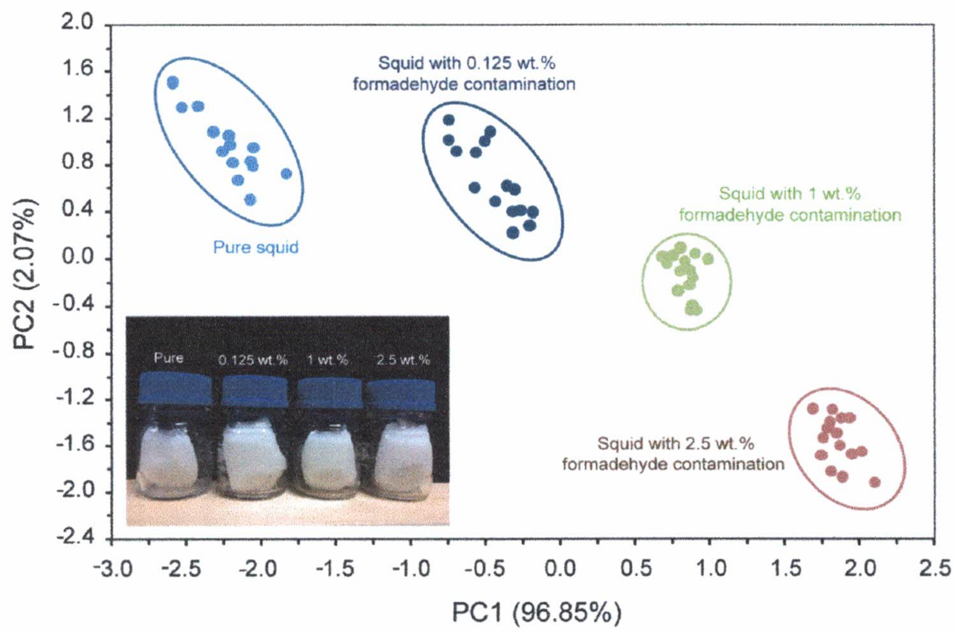

high potential in identification of the formaldehyde contaminated squid samples at room temperature.

4 Conclusion

In conclusion, 2D-hybrid PEDOT:PSS/MWCNTs, PEDOT:PSS/MWCNTs-NH_2 and PEDOT:PSS/MWCNTs-N_2 gas sensors were successfully fabricated by low-cost inkjet printing technique. The SEM shows no significant difference in surface morphology. FTIR characterization confirms the presence of N_2 and NH_2 functional groups of CNTs in PEDOT:PSS polymer matrix after printing on interdigitated silver electrodes. From gas sensing results, PEDOT:PSS/MWCNTs-N_2 sensor exhibits the highest response and selectivity to formaldehyde gas compared with ethanol, methanol, ammonia, nitrogen dioxide and hydrogen sulfide at room temperature. The sensing mechanism of the three fabricated sensors was proposed based on direct charge transfer process. The SCC-DFTB calculation shows a good agreement with experimental results in which CNTs-N_2 exhibits the highest interaction to formaldehyde molecule and changing of electronics properties. For E-nose measurement, response values of the three fabricated sensors to odors of pure and formaldehyde contaminated squid samples were analyzed by PCA method. The PCA result confirms that the three printed sensors can detect and classify the pure and contaminated squids with varying the formalin contaminations. According to the results, the proposed technique for fabrication of formaldehyde gas sensors to identify formalin concentrations in squids offers several advantages over the current typical chemical methods including fast, room temperature operation, simple, no chemical waste, low cost and nondestructive measurement.

Acknowledgements This work was financially supported by the National Research Council of Thailand (NRCT).

References

1. J. Peng, S. Wang, Correlation between microstructure and performance of Pt/TiO_2 catalysts for formaldehyde catalytic oxidation at ambient temperature: effects of hydrogen pretreatment. J. Phys. Chem. C **111**, 9897–9904 (2007)
2. K. Sexton, J.L. Adgate, S.J. Mongin, G.C. Pratt, G. Ramachandran, T.H. Stock, M.T. Morandi, Evaluating differences between measured personal exposures to volatile organic compounds and concentrations in outdoor and indoor air. Environ. Sci. Technol. **38**, 2593–2602 (2004)
3. Y.Y. Maruo, J. Nakamura, Portable formaldehyde monitoring device using porous glass sensor and its applications in indoor air quality studies. Anal. Chim. Acta **702**, 247–253 (2011)
4. Y.M. Zhang, Y.T. Lin, J.L. Chen, J. Zhang, Z.Q. Zhu, Q.J. Liu, A high sensitivity gas sensor for formaldehyde based on silver doped lanthanum ferrite. Sensor. Actuat. B-Chem. **190**, 171–176 (2014)
5. L. Feng, Y. Liu, X. Zhou, J. Hu, The fabrication and characterization of a formaldehyde odor sensor using molecularly imprinted polymers. J. Colloid. Interface Sci. **284**, 378–382 (2005)
6. D. Belpomme, P. Irigaray, L. Hardell, R. Clapp, L. Montagnier, S. Epstein, A.J. Sasco, The multitude and diversity of environmental carcinogens. Environ. Res. **105**, 414–429 (2007)
7. J.H. Arts, M.A. Rennen, C.D. Heer, Inhaled formaldehyde: evaluation of sensory irritation in relation to carcinogenicity. Regul. Toxicol. Pharm. **44**, 144–160 (2006)
8. S. Zhang, C. Xie, Z. Bai, M. Hu, H. Li, D. Zeng, Spoiling and formaldehyde-containing detections in octopus with an E-nose. Food. Chem. **113**, 1346–1350 (2009)
9. Y. Lin, Y. Wang, W. Wei, L. Zhu, S. Wen, S. Ruan, Synergistically improved formaldehyde gas sensing properties of SnO_2 microspheres by indium and palladium co-doping. Ceram. Int. **41**, 7329–7336 (2015)
10. N.V. Hieu, N.A.P. Duc, T. Trung, M.A. Tuan, N.D. Chien, Gas-sensing properties of tin oxide doped with metal oxides and carbon nanotubes: a competitive sensor for ethanol and liquid petroleum gas. Sensor. Actuat. B-Chem. **144**, 450–456 (2010)
11. H. Xie, C. Sheng, X. Chen, X. Wang, Z. Li, J. Zhou, Multi-wall carbon nanotube gas sensors modified with amino-group to detect low concentration of formaldehyde. Sensor. Actuat. B-Chem. **168**, 34–38 (2012)
12. Y.M. Zhang, J. Zhang, J.L. Chen, Z.Q. Zhu, Q.J. Liu, Improvement of response to formaldehyde at Ag–$LaFeO_3$ based gas sensors through incorporation of SWCNTs. Sensor. Actuat. B-Chem. **195**, 509–514 (2014)
13. D. Shi, L. Wei, J. Wang, J. Zhao, C. Chen, D. Xu, H. Geng, Y. Zhang, Solid organic acid tetrafluorohydroquinone functionalized single-walled carbon nanotube chemiresistive sensors for highly sensitive and selective formaldehyde detection. Sensor. Actuat. B-Chem. **177**, 370–375 (2013)
14. K. Zhou, X. Ji, N. Zhang, X. Zhang, On-line monitoring of formaldehyde in air by cataluminescence-based gas sensor. Sensor. Actuat. B-Chem. **119**, 392–397 (2006)
15. X. Chang, X. Wu, Y. Guo, Y. Zhao, J. Zheng, X. Li, $SnSO_4$ modified ZnO nanostructure for highly sensitive and selective formaldehyde detection. Sensor. Actuat. B-Chem. **255**, 1153–1159 (2018)
16. A. Pantano, D.M. Parks, M.C. Boyce, Mechanics of deformation of single- and multi-wall carbon nanotubes. J. Mech. Phys. Solids **52**, 789–821 (2014)
17. K. Balasubramanian, M. Burghard, Chemically functionalized carbon nanotubes. Small **1**, 180–192 (2005)
18. G.J. Cadena, J. Riu, F.X. Rius, Gas sensors based on nanostructured materials. Analyst **132**, 1083–1099 (2007)
19. C.K. Liu, C.T. Hu, Y.H. Yang, Y.S. Chang, H.C. Shih, Synthesis, characterization and field emission of single wall carbon nanotubes. Diamond. Relat. Mater. **18**, 345–350 (2009)
20. J. Kong, N.R. Franklin, C. Zhou, M.G. Chapline, S. Peng, K. Cho, H. Dai, Nanotube molecular wires as chemical sensors. Science **287**, 622–625 (2000)
21. J. Suehiro, H. Imakiire, S.I. Hidaka, W. Ding, G. Zhou, K. Imasaka, M. Hara, Schottky-type response of carbon nanotube NO_2 gas sensor fabricated onto aluminum electrodes by dielectrophoresis. Sensor. Actuat. B-Chem. **114**, 943–949 (2006)
22. C. Cantalini, L. Valentini, I. Armentano, L. Lozzi, J.M. Kenny, S. Santucci, Sensitivity to NO_2 and cross-sensitivity analysis to NH_3, ethanol and humidity of carbon nanotubes thin film prepared by PECVD. Sensor. Actuat. B-Chem. **95**, 195–202 (2003)
23. C.D. Kim, H.R. Lee, H.T. Kim, Effect of NH3 gas ratio on the formation of nitrogen-doped carbon nanotubes using thermal chemical vapor deposition. Mater. Chem. Phys. **183**, 315–319 (2016)

24. B. Wang, X. Zhou, Y. Wu, Z. Chen, C. He, Lead phthalocyanine modified carbon nanotubes with enhanced NH_3 sensing performance. Sensor. Actuat. B-Chem. **171–172**, 398–404 (2012)
25. L. Valentini, C. Cantalini, L. Lozzi, S. Picozzi, I. Armentano, J.M. Kenny, S. Santucci, Effects of oxygen annealing on cross sensitivity of carbon nanotubes thin films for gas sensing applications. Sensor. Actuat. B-Chem. **100**, 33–40 (2004)
26. D. Jana, C.L. Sun, L.C. Chen, K.H. Chen, Effect of chemical doping of boron and nitrogen on the electronic, optical, and electrochemical properties of carbon nanotubes. Prog. Mater Sci. **58**, 565–635 (2013)
27. A.M. Nardes, M. Kemerink, M.M. de Kok, E. Vinken, K. Maturova, R.A.J. Janssen, Conductivity, work function, and environmental stability of PEDOT:PSS thin films treated with sorbitol. Org. Electron. **9**, 727–734 (2008)
28. A.S. Abdullah, M.R. Alenezi, K.T. Lai, S.R.P. Silva, Inkjet printing of polymer functionalized CNT gas sensor with enhanced sensing properties. Mater Lett. **189**, 299–302 (2017)
29. D.J. Late, Y.K. Huang, B. Liu, J. Acharya, S.N. Shirodkar, J. Luo, A. Yan, D. Charles, U.V. Waghmare, V.P. Dravid, C.N.R. Rao, Sensing behavior of atomically thin-layered MoS_2 transistors. ACS Nano **7**, 4879–4891 (2013)
30. M.B. Erande, M.S. Pawar, D.J. Late, Humidity sensing and photodetection behavior of electrochemically exfoliated atomically thin-layered black phosphorus nanosheets. ACS Appl. Mater. Interfaces **8**, 11548–11556 (2016)
31. M. Pawar, S. Kadam, D.J. Late, High-performance sensing behavior using electronic ink of 2D $SnSe_2$ nanosheets. Chem. Select. **2**, 4068–4075 (2017)
32. P.K. Kannan, D.J. Late, H. Morgan, C.S. Rout, Recent developments in 2D layered inorganic nanomaterials for sensing. Nanoscale **7**, 13293–13312 (2015)
33. Y. Seekaew, S. Lokavee, D. Phokharatkul, A. Wisitsoraat, T. Kerdcharoen, C. Wongchoosuk, Low-cost and flexible printed graphene–PEDOT:PSS gas sensor for ammonia detection. Org. Electron. **15**, 2971–2981 (2014)
34. K. Timsorn, T. Thoopboochagorn, N. Lertwattanasakul, C. Wongchoosuk, Evaluation of bacterial population on chicken meats using a briefcase electronic nose. Biosyst. Eng. **151**, 116–125 (2016)
35. K. Timsorn, Y. Lorjaroenphon, C. Wongchoosuk, Identification of adulteration in uncooked Jasmine rice by a portable low-cost artificial olfactory system. Measurement **108**, 67–76 (2017)
36. S. Balasubramanian, S. Panigrahi, C.M. Logue, H. Gu, M. Marchello, Neural networks-integrated metal oxide-based artificial olfactory system for meat spoilage identification. J. Food. Eng. **91**, 91–98 (2009)
37. N.E. Barbri, E. Llobet, N.E. Bari, X. Correig, B. Bouchikhi, Electronic nose based on metal oxide semiconductor sensors as an alternative technique for the spoilage classification of red meat. Sensors **8**, 142–156 (2008)
38. C. Wongchoosuk, A. Wisitsoraat, A. Tuantranont, T. Kerdcharoen, Portable electronic nose based on carbon nanotube-SnO_2 gas sensors and its application for detection of methanol contamination in whiskeys. Sensor. Actuat. B-Chem. **147**, 392–399 (2010)
39. Z. Yang, F. Dong, K. Shimizu, T. Kinoshita, M. Kanamori, A. Morita, N. Watanabe, Identification of coumarin-enriched Japanese green teas and their particular flavor using electronic nose. J. Food. Eng. **92**, 312–316 (2009)
40. H. Yu, J. Wang, H. Xiao, M. Liu, Quality grade identification of green tea using the eigenvalues of PCA based on the E-nose signals. Sensor. Actuat. B-Chem. **140**, 378–382 (2009)
41. C. Wongchoosuk, K. Subannajui, C. Wang, Y. Yang, F. Guder, T. Kerdcharoen, V. Cimalla, M. Zacharias, Electronic nose for toxic gas detection based on photostimulated core–shell nanowires. RSC. Adv. **4**, 35084–35088 (2014)
42. X. Li, Y. He, C. Wu, Non-destructive discrimination of paddy seeds of different storage age based on Vis/NIR spectroscopy. J. Stored Prod. Res. **44**, 264–268 (2008)
43. P. Lorwongtragool, E. Sowade, N. Watthanawisuth, R.R. Baumann, T. Kerdcharoen, A novel wearable electronic nose for healthcare based on flexible printed chemical sensor array. Sensors **14**, 19700–19712 (2014)
44. M. Ringner, What is principal component analysis. Nat. Biotechnol. **26**, 303–304 (2008)
45. M. Elstner, The SCC-DFTB method and its application to biological systems. Theor. Chem. Acc. **116**, 316–325 (2006)
46. A. Marutaphan, Y. Seekaew, C. Wongchoosuk, Self-consistent charge density functional tight-binding study of poly(3,4-ethylenedioxythiophene):poly(styrenesulfonate) ammonia gas sensor. Nanoscale. Res. Lett. (2017). https://doi.org/10.1186/s11671-017-1878-2
47. H. Soleymanabadi, J. Kakemam, A DFT study of H_2 adsorption on functionalized carbon nanotubes. Physica E **54**, 115–117 (2013)
48. M.D. Ganji, A. Bakhshandeh, Functionalized single-walled carbon nanotubes interacting with glycine amino acid: DFT study. Physica B **406**, 4453–4459 (2011)
49. L. Stobinski, B. Lesiak, L. Kover, J. Toth, S. Biniak., G. Trykowski, J. Judek, Multiwall carbon nanotubes purification and oxidation by nitric acid studied by the FTIR and electron spectroscopy methods. J. Alloy. Compd. **501**, 77–84 (2010)
50. E. Ghasemy, H.B. Motejadded, A. Rashidi, T. Hamzehlouyan, Z. Yousefian, N-doped CNT nanocatalyst prepared from camphor and urea for gas phase desulfurization: experimental and DFT study. J. Taiwan. Inst. Chem Eng. **000**, 1–11 (2018)
51. L.R. Tsai, M.H. Chen, C.T. Chien, M.K. Chen, F.S. Lin, K.M.C. Lin, Y.K. Hwu, C.S. Yang, S.Y. Lin, A single-monomer derived linear-like PEI-co-PEG for siRNA delivery and silencing. Biomaterials **32**, 3647–3653 (2011)
52. Y. Zhu, H. Li, Q. Zheng, J. Xu, X. Li, Amine-functionalized SBA-15 with uniform morphology and well-defined mesostructure for highly sensitive chemosensors to detect formaldehyde vapor. Langmuir **28**, 7843–7850 (2012)
53. A. Maleki, U. Hamesadeghi, H. Daraei, B. Hayati, F. Najafi, G. Mckay, R. Rezaee, Amine functionalized multi-walled carbon nanotubes: single and binary systems for high capacity dye removal. Chem. Eng. J. **313**, 826–835 (2017)
54. S.A. Boampong, J.J. Belbruno, Detection of formaldehyde vapor using conductive films. Sensor. Actuat. B-Chem. **182**, 300–306 (2013)
55. V.S. Vaishnav, S.G. Patel, J.N. Panchal, Development of ITO thin film sensor for the detection of formaldehyde at room temperature. Sensor. Actuat. B-Chem. **202**, 1002–1009 (2014)
56. M. Yoosefian, H. Raissi, A. Mola, The hybrid of Pd and SWCNT (Pd loaded on SWCNT) as an efficient sensor for the formaldehyde molecule detection: a DFT study. Sensor. Actuat. B-Chem. **212**, 55–62 (2015)